**Research Article** **Open Access**

W. Changcharoen, P. Somravysin, and S. Eiamsa-ard*

# Thermal and fluid flow characteristics in a tube equipped with peripherally-cut dual twisted tapes

**Abstract:** This article presents an experimental analysis of the turbulent flow of water in a heat exchanger tube fitted with peripherally-cut dual twisted tapes (PDTs) under a constant wall heat-flux condition. The peripherally-cut dual twisted tapes with different cutting pitch ratios ($l/y$ = 0.5, 0.75 and 1.0) were tested for Reynolds numbers in the range of 5400 to 14,000. The experimental results showed that Nusselt number and friction factor of the tubes fitted with PDTs were considerably higher than those of the plain tube and those of the tubes with single twisted tape (ST) and dual twisted tapes (DTs). It was found that PDTs with $l/y$ = 0.5, 0.75 and 1.0 gave higher heat transfer rate than the typical DTs, with average Nusselt numbers greater by 12.1%, 7.8% and 3.8%, respectively. For the range investigated, PDTs with the smallest $l/y$ ratio offered the highest thermal performance factor of 1.14.

**Keywords:** Heat transfer augmentation, Heat exchanger, Swirl flow, Turbulent flow, Twisted tape, Peripherally-cut dual twisted tapes

DOI 10.1515/eng-2015-0009
Received September 09, 2014; accepted November 04, 2014

## 1 Introduction

Numerous techniques have been developed to improve heat transfer in heat exchanger systems for economic and sustainability reasons [1, 2]. Several numerical studies on the optimization of heat transfer in a tube/pipe/channel under different heat flux have been carried out. Hajmohammadi et al. [3] optimized heat transfer and fluid flow in partially curved pipes. Their results demonstrated that the partially curved pipe (three straight pipe segments connected with two 90° bends) could reduce pressure drop and entropy generation rate by up to 11% and 160%, respectively, as compared to the fully curved tubes. Hajmohammadi et al. [4] applied constructal theory to enhance the heat transfer from a discretely heated pipe by placing a sequence of insulated segments between heated segments in a tube wall. They found that the optimal location of the insulated segments, along with the reduction of the peak temperature, was strongly dependent on Graetz number. At moderate Graetz numbers, the peak temperatures were remarkably reduced in response to the optimal placement of the insulated/heated segments. In addition, Hajmohammadi et al. [5] optimized the distribution of heat flux for heat transfer enhancement in a round pipe for both fully-developed and developing laminar flow. Their numerical results implied that the optimum distribution of heat flux, which minimized the peak temperature, corresponded with the 'descending' distribution. Recently, Hajmohammadi et al. [6] carried out the optimal design of the heat flux elements fitted on the outer walls of a rectangular duct in order to minimize the hot spot temperature. They found that the hot spot temperature could be reduced by up to 25% in the case of four unequal heat flux elements, under the influence of intermediate values of Graetz number.

Heat transfer enhancement techniques are widely applied in many fields, including chemical processing, electric power generation, steam generation, waste heat recovery, environmental protection, etc. Inserting twisted tape is one of the most widely adopted techniques. Typically, a twisted tape creates one or more combinations of the following conditions that are favorable for the augmentation of heat transfer: 1) spiral/swirling/rotating and/or secondary flows, which increase turbulence intensity; 2) gross flow mixing, which leads to the disruption of the developing thermal/velocity boundary layer, and; 3) increase in heat transfer area. It also does, however, lead to an undesirable rise of friction.

The heat transfer augmentation using twisted tapes with different geometries/arrangements has been extensively investigated. Guo et al. [7] conducted a comparative study on heat transfer enhancement by center-cleared twisted tape and typical twisted tapes. It was found that the ther-

**W. Changcharoen, P. Somravysin:** Department of Mechanical Engineering, Faculty of Engineering, Mahanakorn University of Technology, Bangkok 10530, Thailand
***Corresponding Author: S. Eiamsa-ard:** Department of Mechanical Engineering, Faculty of Engineering, Mahanakorn University of Technology, Bangkok 10530, Thailand, E-mail: smith@mut.ac.th

mal performance factor of the tube with center-cleared twisted tape was enhanced by up to 20% over that of the typical twisted tape. Bas and Ozceyhan [8] conducted experiments to study the flow friction and heat transfer behavior in a circular tube fitted with loose-fitted twisted tapes with different twist and clearance ratios. Their results showed that the heat transfer performance increased with the decreasing twist and clearance ratios. The heat transfer enhancement was evaluated based on equal pumping power. The maximum heat transfer enhancement of 1.756 times, as compared to that of the plain tube, was achieved by using tape with clearance ratio of 0.0178 and twist ratio of 2.0.

Eiamsa-ard et al. [9] investigated the heat transfer enhancement using twisted tapes with alternate axes at different alternate lengths. Effects of uniform and non-uniform alternate lengths were also reported and compared with those of typical twisted tape. It was found that the twisted tapes with alternate axes at alternate length of 0.5 gave the highest heat transfer, friction factor and thermal performance factor. Eiamsa-ard et al. [10] reported the influence of twin-counter/co-twisted tapes on heat transfer enhancement. As found, the counter-twisted tapes gave heat transfer augmentation up to 44.5% over those given by the co-twisted tapes.

Eiamsa-ard and Wongcharee [11] showed the combined influence of nanofluids, dual twisted-tapes (DTs) and a micro-fin tube (MF) on thermal performance factor behaviors. The CuO-water nanofluid concentration was varied from 0.3% to 1.0% by volume. Markedly, the combined techniques offered superior thermal performance factor over the individual techniques. In addition, thermal performance increased with increasing nanofluid concentration.

Hong et al. [12] numerically investigated the flow and heat transfer characteristics in converging-diverging tubes (CDs) and in CDs equipped with twin counter-swirling twisted tapes (CDTs). Effects of the pitch length, rib height, pitch ratio, gap distance between twin twisted tapes and tape number on thermal enhancement factor were examined. They found that heat transfer and friction factor given by CDT were higher than those given by bare CD, up to 35.7% and 5.3 times higher, respectively. In addition, all CDTs possessed thermal performance factor greater than unity for the entire studied range.

Promvonge et al. [13] studied the heat transfer enhancement in a helical-ribbed tube fitted with twin twisted tapes. Effects of single rib-height to tube-diameter ratio ($e/D_H$), rib-pitch to diameter ratio ($P/D_H$) of helical-ribbed tube, and twist ratio on thermal performance were investigated. The experimental results revealed that the helical-ribbed tube with twin twisted tapes performed better than the ribbed tube alone.

Eiamsa-ard and Wongcharee [14] examined the thermal performance factor in a micro-fin tube with double twisted-tape inserts at different configurations: (1) twisted tapes actingin the same direction (for co-swirl),with micro-fin tube and twisted tapes acting in the same (parallel) direction (MF-CoDTs:P); (2) twisted tapes acting in the same direction (for co-swirl),with micro-fin tube and twisted tapes acting in opposite direction (MF-CoDTs:O), and; (3) twisted tapes acting in opposite directions for counter swirls(MF-CDTs). Thermal performance factors associated with the use of MF-CDTs were found to be higher than those associated with the uses of MF-CoDTs:P, MF-CoDTs:O and MF alone: up to 9.3%, 6.5% and 56.4% higher, respectively.

Bhuiya et al. [15] studied the influence of the double counter twisted tapes on heat transfer and fluid friction characteristics in a heat exchanger tube at different twist ratios ($y$ = 1.95, 3.85, 5.92 and 7.75) using air as the working fluid. They found that the heat transfer performance and friction factor of the tube with double counter twisted tapes were, respectively, 240% and 286% higher than those of the plain tube. In addition, thermal performance factor achieved by the use of the tapes was as high as 1.34.

The results reported in this literature review indicate that heat transfer enhancement, pressure drop and thermal performance factor characteristics are strongly dependent on geometrical properties of twisted tapes. The present work proposes alternative modified twisted tapes: namely, peripherally-cut dual twisted tapes (PDTs) with three different cutting pitchratios ($l/y$ = 0.5, 0.75 and 1.0). The PDTs contain gaps in the peripheral region of the tapes. The gaps are generated in order to induce additional turbulence, especially in the vicinity of the tube wall. Thermal performance factors were evaluated based on equal pumping power for both tubes with and without tape. The typical single and dual twisted tapes (ST and DTs) were also tested for comparison purpose. The present research also aims to formulate the empirical correlations for predicting Nusselt number, friction factor and thermal performance factor of the tubes equipped with PDTs.

## 2 Peripherally-cut dual twisted tapes (PDTs)

Three types of twisted tapes include typical single twisted tape (ST), typical dual twisted tapes (DTs), and newly de-

veloped peripherally-cut dual twisted tapes (PDTs). These were prepared for comparative investigation as shown in Figure 1. Each twisted tape was made from an aluminum straight sheet with tape length ($L$) of 1000 mm and tape thickness ($\delta$) of 0.8 mm. The tape thickness of 0.8 mm was chosen as an optimum one. Thinner tape can be torn easily during the twisting operation, while thicker tape can cause large friction in the system. The widths ($W$) of ST, one of DTs and one of PDTs, were 9, 8, and 19 mm, respectively. To fabricate a typical twisted tape, one end of a straight tape was clamped while another end was carefully twisted to obtain a desired twist length. All tapes were prepared with constant twist ratio, $y/W = 3.0$, defined as the twist length (180°/twist length) to the width ($W$) of each tape. To formulate DTs and PDTs, two tapes were welded together using a small aluminum wire. To obtain the PDTs, the DTs were modified by cutting on the edges of tapes at constant depth of cut ratio ($d/W = 0.33$). The $l/y$ ratio,defined as the ratio of the cutting pitch ($l$) to the twist length ($y$, 180°/twist length), was varied from 0.5 to 1.0 ($l/y = 0.5$, 0.75 and 1.0).Note that for DTs and PDTs, the tapes were aligned to generate swirl flow in the same direction (*co-swirl flow*).

# 3 Details of experimental apparatus

The schematic diagram of the experimental rig is presented in Figure 2. The system consists of: (1) a heating tube with insulator; (2) thermocouples for measuring the fluid and the tube wall temperatures; (3) a data logger connected to a personal computer; (4) a variac transformer for controlling the electrical power output to the test section; (5) an amp/volt meter; (6) a centrifugal water pump; (7) a water chiller; (8) two water tanks, positioned at the bottom and at the top of the heating section; (9) a rotameter for measuring the volumetric water flow rate; (10) two pressure taps for measuring the pressure drop across the test section; (11) a mixing chamber located at the end of the heating section; (12) a calm section with the length of 1500 mm (or 83D) connected to the entrance of the heating section, for ensuring the fully developed flow of the entering fluid. More details of the experimental setup and procedure have been described elsewhere [10]. In the experiments, the Reynolds number of the water was varied between 5400 and 14,000. The Prandtl number values were calculated based on the bulk flow temperature ($T_b = \frac{T_i+T_o}{2}$). The inlet temperature ($T_i$) was maintained at 26°C,and the outlet temperature ($T_o$) could rise up to 37°C, depending on operating conditions. During the tests, fifteen local temperatures of the tube wall were measured using type-T thermocouples, while the inlet and outlet fluid temperatures were measured by resistance temperature detectors (RTDs). All temperature data were recorded by the data logger. The pressure drop across the test length was measured with a digital manometer using water as a working fluid. One tap of the manometer was placed 2.5D upstream of the entrance of the test tube, while the other tap was located 6D downstream of the exit of the test tube. To ensure steady-state for each condition, a period of around 25 to 50 minutes was allowed to pass prior to the data record, depending on the Reynolds number and tape shape.

# 4 Data reduction

## 4.1 Heat transfer and pressure loss

The heat transfer and pressure loss results in the tube with or without peripherally-cut dual twisted tapes (PDTs) inserts were taken according to the experimental procedure described in the previous section. During the tests, water in the test section received heat ($Q_w$) from the electrical heat wire mainly via the convective heat transfer mechanism. Thereby, the $eQ_w$ is assumed to be equal to the convective heat transfer within the test section, which can be written as:

$$Q_w = Q_c \tag{1}$$

The heat gained by the water in terms of enthalpy change can be expressed as:

$$Q_w = MC_{p,w}(T_o - T_i) \tag{2}$$

In the experiments, the heat equilibrium test showed that the heat received by the water ($Q_w$) is between 4 and 7% lower than that supplied by electrical heating ($Q_{VI} = IV$) under uniform heat flux condition (UHF). This is due to the heat loss from the tube wall.

$$\frac{(Q_{VI} - Q_w) \times 100\%}{Q_{VI}} = 4 - 7\% \tag{3}$$

The average value of heat absorbed by the fluid is taken from internal convective heat transfer coefficient calculation by the following equation:

$$Q_w = Q_c = hA(\tilde{T}_s - T_b) \tag{4}$$

where $A$ is the internal surface of the tube wall ($\pi DL$) and $T_b$ is the mean bulk flow temperature:

$$T_b = \frac{T_o + T_i}{2} \tag{5}$$

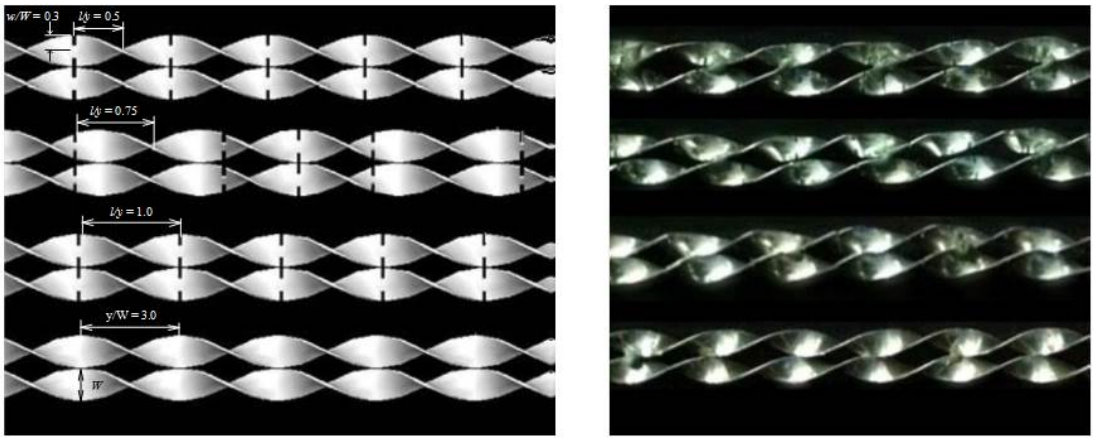


**Figure 1:** Dimensional parameters and photographs of peripherally-cut dual twisted tapes (PDTs) and dual twisted tapes (DTs).

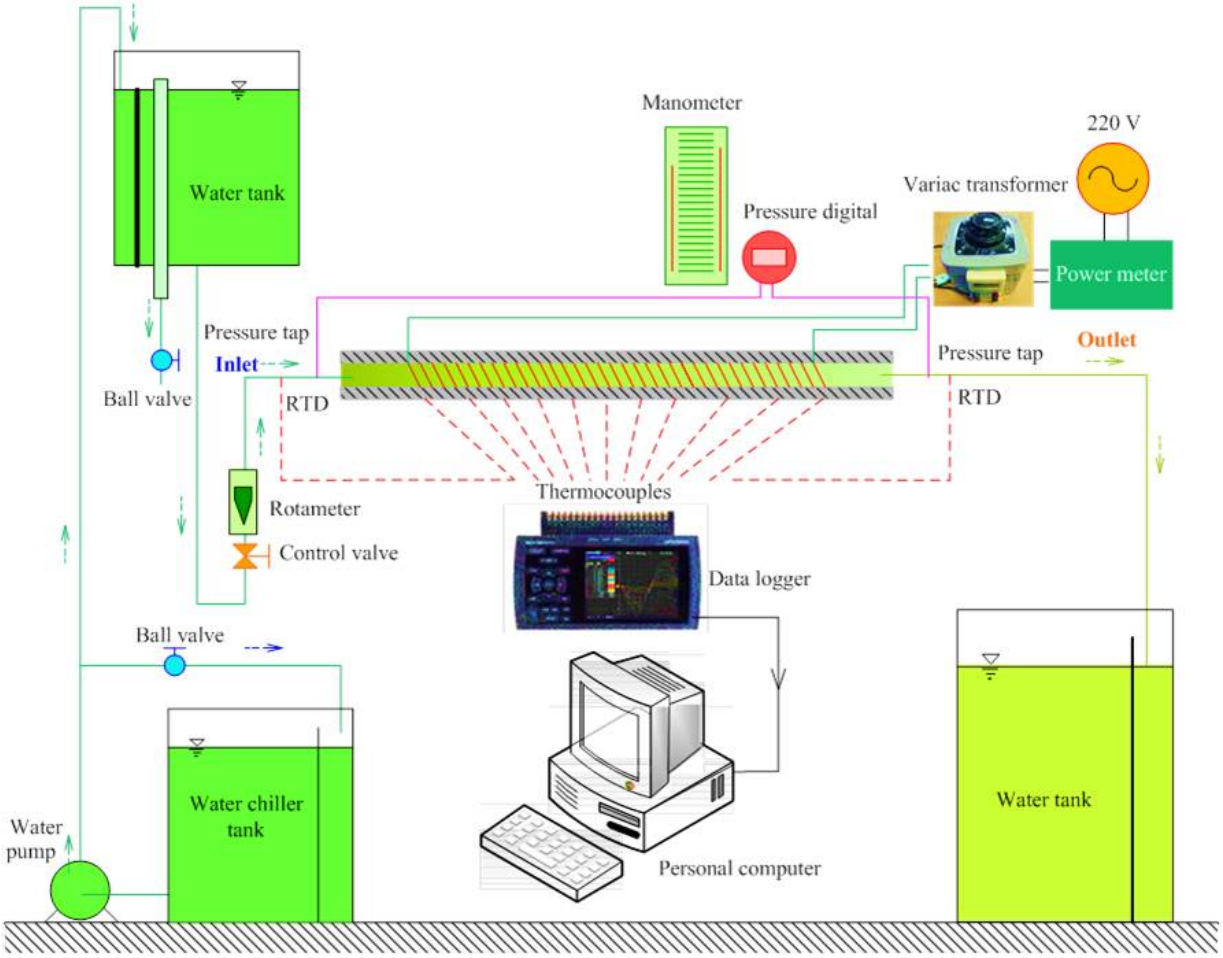


**Figure 2:** Experimental heat transfer set-up.

The mean inner wall surface temperature ($\tilde{T}_s$ of the test tube is calculated from 15 stations of surface temperatures ($T_s$) lined between the inlet and the exit of the test tube, using the following equation:

$$\tilde{T}_s = \Sigma T_s/15 \tag{6}$$

Mean convective heat transfer coefficient ($h$) can be calculated using Eq. (4) and mean Nusselt number ($Nu$) is then estimated from Eq.(7):

$$Nu = \frac{hD}{k} \tag{7}$$

The flow regime can be defined from the Reynolds number ($Re$):

$$Re = \frac{\rho UD}{\mu} \tag{8}$$

All the fluid thermo-physical properties of the water were determined based on the mean bulk fluid temperature ($T_b$). In the experiments, pressure losses across the test section with and without twisted tapes were measured. The friction factors are then obtained by the following equation:

$$f = \frac{\Delta P}{\left(\frac{L}{D}\right)\rho\frac{U^2}{2}} \tag{9}$$

## 4.2 Experimental uncertainty

In the present work, the experimental uncertainty was estimated using the method of Moffat [16, 17]. The uncertainty of any independent variable can be expressed as:

$$\delta RX_i = \frac{\partial R}{\partial X_i}\delta X_i \tag{10}$$

When several independent variables are used in the function $R$, the individual terms are combined by root-sum-square method:

$$\delta R = \left\{\sum_{i=1}^{N}\left(\frac{\partial R}{\partial X_i}\delta X_i\right)^2\right\}^{\frac{1}{2}} \tag{11}$$

The individual factors denoted by $x_i$, can be used for uncertainty evaluation of a dependent variable as:

$$w(k, h, D, f, U, \ldots) = \left[(x_1)^2 + (x_2)^2 + \ldots + (x_N)^2\right]^{\frac{1}{2}} \tag{12}$$

For example, the uncertainty of the Nusselt number can be calculated by combinations of Eqs. (7) and (12) as:

$$w_{Nu} = \left[\left(\frac{\partial Nu}{\partial h}w_h\right)^2 + \left(\frac{\partial Nu}{\partial D}w_D\right) + \left(\frac{\partial Nu}{\partial k}w_k\right)\right]^{\frac{1}{2}} \tag{13}$$

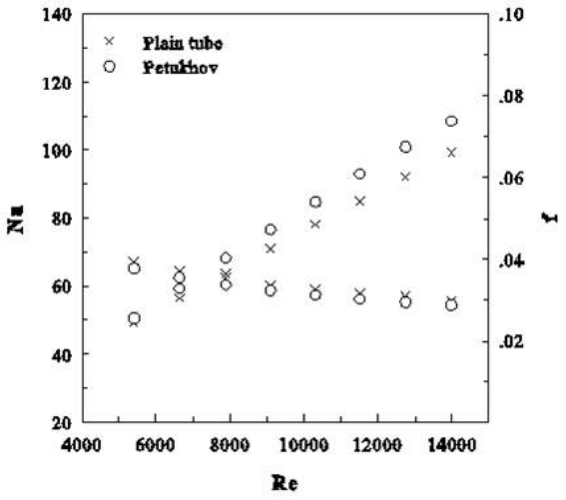


**Figure 3:** Data verification of mean Nusselt number and friction coefficient for the plain tube.

$$\frac{w_{Nu}}{Nu} = \left[\left(\frac{w_h}{h}\right)^2 + \left(\frac{w_D}{D}\right)^2 + \left(\frac{w_k}{k}\right)^2\right]^{\frac{1}{2}} \tag{14}$$

The maximum uncertainty values of the present experimental data for Nusselt number, friction factor and Reynolds number are 7.8%, 8.5% and 6.4%, respectively.

# 5 Experimental results and discussion

## 5.1 Verification of plain tube

The verification was carried out by comparing the results of the plain tube (the tube without twisted tape) in the present work with those calculated from the standard correlations. The standard correlations of Nusselt number and friction factor, given by Petukhov [18] for the fully developed turbulent flow in a round tube are stated below:

$$Nu = \frac{(f/8)RePr}{1.07 + 12.7\sqrt{f/8}(Pr^{2/3} - 1)}\left(\frac{\mu_b}{\mu_w}\right)^{0.11} \tag{15}$$

The comparisons are demonstrated in Figure 3. Evidently, the present experimental data are in good agreement with the Petukhov correlations, within ±6.8% for Nusselt number and within ±4.2% for the friction factor. This indicates hat the experimental data are reliable, providing the confidence to use the present experimental facility for further experiments with tube inserts.

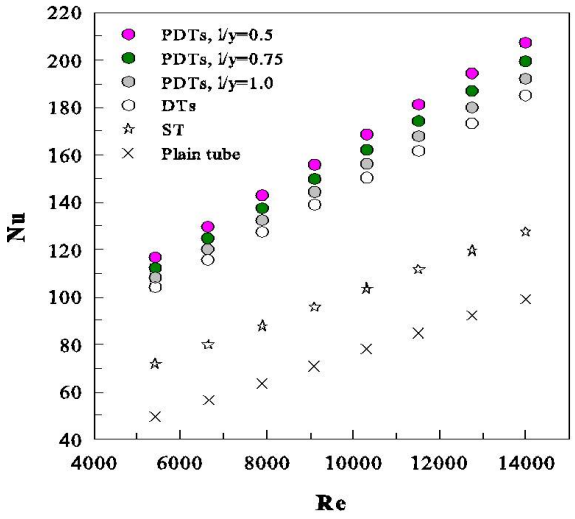


**Figure 4:** Nusselt number against Reynolds number for PDTs at various cutting pitch ratios ($l/y$ = 0.5, 0.75 and 1.0).

## 5.2 Heat transfer

The variation of heat transfer performance (expressed by the Nusselt number) and Reynolds number ($Re$) is shown in Figure 4. The results of the tubes fitted with PDTsat three different cutting pitch ratios ($l/y$ = 0.5, 0.75 and 1.0) are compared with those of the tubes with ST and DTs, as well as the plain tube. In general, the Nusselt number considerably increased with the rise of Reynolds number. At a given $Re$, the Nusselt number in the tubes with PDTs were higher than those with ST, DTs and also the plain tube.

Numerical results in Figure 5 reveal that recirculation flows causing dead zones appeared near the tube wall of the tube with DTs, while such flows did not appear in the tube with PDTs. This indicates that apart from common swirl flow, PDTsalso induced extra turbulence around peripheral cuts. The effect of the extra turbulence by PDTs results in stronger turbulence intensity (Figure 6), and better fluid mixing between core and tube wall region, leading to more efficient heat transfer enhancement as compared to DTs. This is revealed by comparison of the distributions of the local Nusselt numbers in the tubes fitted with PDTs and DTs at $Re$ = 20, 000 (Figure 7). The effects of extra turbulence on further heat transfer enhancement are in agreement with the results of Eiamsa-ard and Wongcharee [11], Promvonge et al. [13] and Eiamsa-ard and Wongcharee [14]. For the PDTs, heat transfer enhancement increased with decreasing cutting pitch ratio(or increasing number of cuts), due to the increasing frequency of the additional flow disturbance along the test tubes. According to the experimental results, the average Nusselt numbers given by

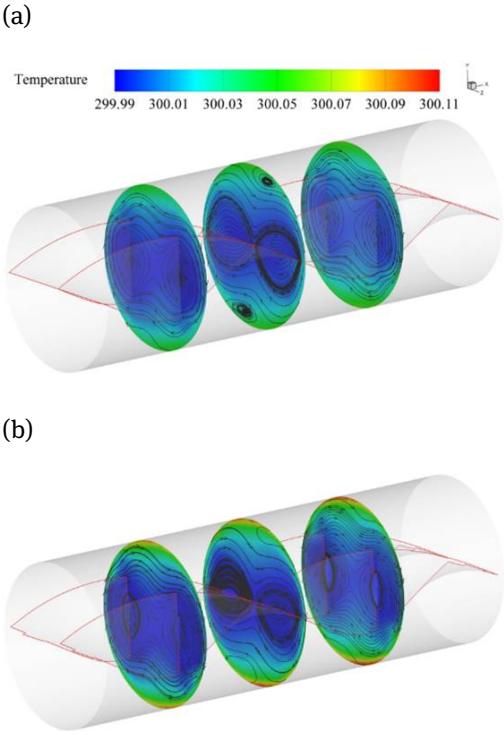


**Figure 5:** Streamline and fluid temperature in cross-section view of tapes: (a) dual twisted tapes (DTs); (b) peripherally-cut dual twisted tapes (PDTs: $l/y$ = 0.5).

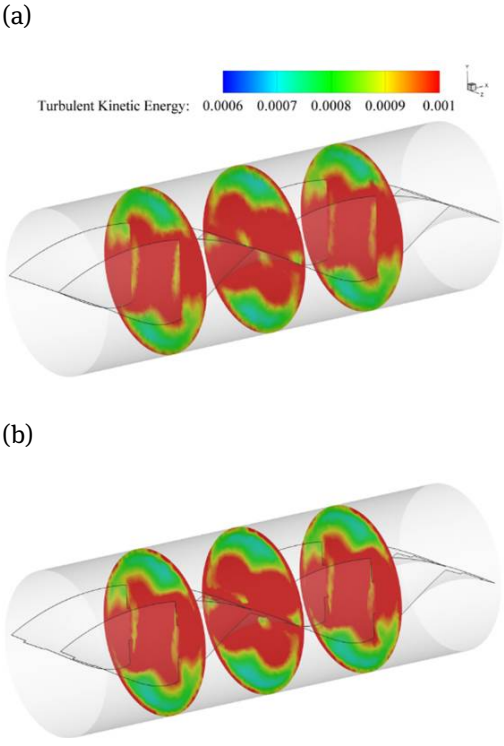


**Figure 6:** Turbulent kinetic energy (TKE) in cross-section view of tapes: (a) dual twisted tapes (DTs); (b) peripherally-cut dual twisted tapes (PDTs: $l/y$ = 0.5).

(a)

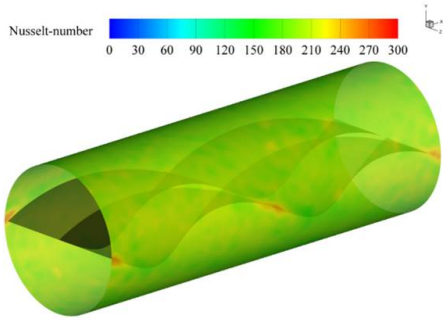


(b)

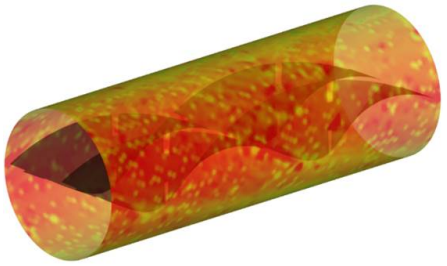

**Figure 7:** Distribution of local Nusselt number around the tube: (a) dual twisted tapes (DTs); (b) peripherally-cut dual twisted tapes (PDTs: $l/y = 0.5$).

PDTs with $l/y = 0.5$, 0.75 and 1.0 were, respectively, 62.5%, 56.4% and 50.6% higher than those given by ST, and 12.1%, 7.8% and 3.8% higher than those given by DTs. In other words, PDTs with $l/y = 0.5$ offered 3.9% and 7.9% higher heat transfer than the ones with $l/y = 0.75$ and 1.0, respectively. As compared to the plain tube, the tube with PDTs with the smallest cutting pitch ratio ($l/y = 0.5$) enhanced heat transfer by 109 to 136%, for the Reynolds number ranging from 5400 to 14,000.

## 5.3 Friction factor

The variation of friction factor with Reynolds number, for the considered cases, is shown in Figure 8. Friction factor tended to decrease with increasing Reynolds number. At the same Reynolds number, the tubes with PDTs possessed higher friction factors than the ones with ST, DTs or the plain tube. This is attributed to the higher dissipation of dynamic pressure caused by the swirl flow, as well as additional flow disturbance around peripheral cuts, as compared to those caused by common swirls (in the tubes with ST and DTs) or only axial flow (in the plain tube). The average friction factors of the tubes with PDTs at $l/y = 0.5$,

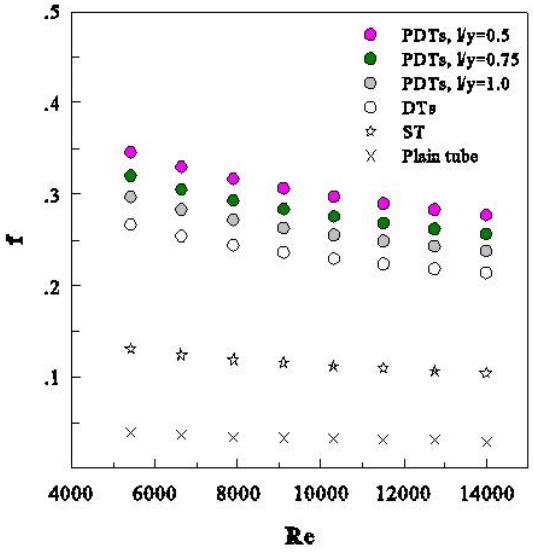


**Figure 8:** Friction factor against Reynolds number for PDTs at various cutting pitch ratios ($l/y = 0.5$, 0.75 and 1.0).

0.75 and 1.0 were, respectively, 9.1, 8.4, 7.8 times those of the plain tube, 2.65, 2.45, 2.27 times of those one with ST, and 1.29, 1.20, 1.11 times those with DTs.

For PDTs, friction factor increased as cutting pitch ratio decreased. As compared to the PDTs with $l/y = 0.75$ and 1.0, the ones with the smallest cutting pitch ratio ($l/y = 0.5$) generated higher friction factor, up to 1.08 times and 1.16 times greater. This can be explained by the same reason proposed for Nusselt number; that is, that the decrease of cutting pitch ratio results in the increase of frequency of the additional flow disturbance, which thus increases friction loss.

## 5.4 Thermal performance criteria

The thermal performance factors were evaluated based on equal pumping power for tubes with and without tape insert [19]. Thermal performance factor above unity indicates that applying peripherally-cut dual twisted tapes (PDTs) for heat transfer enhancement results in net energy gain, and thus operational expense savings. For constant pumping power condition:

$$(V\Delta P)_p = (V\Delta P)_t \tag{16}$$

The relationship between friction factor and Reynolds number can be expressed as:

$$(fRe^3)_p = (fRe^3)_t \tag{17}$$

The thermal performance factor ($\eta$) at constant pumping power is the ratio of the convective heat transfer coefficient of the tube with PDTs to that of the plain tube, which can be written as follows:

$$\eta = \left.\frac{h_t}{h_p}\right|_{pp} \tag{18}$$

The relationship between thermal performance factor ($\eta$) versus Reynolds number is shown in Figure 9. Evidently, thermal performance factor decreases with increasing Reynolds number. At a given Reynolds number, PDTs and DTs gave comparable thermal performance factors, which were significantly higher than those given by ST. For PDTs, thermal performance factor increased with decreasing cutting pitch ratio. The PDTs with $l/y$ = 0.5, 0.75 and 1.0 offered thermal performance factors between 0.99 and 1.14,0.98 and 1.13, and 0.97and 1.11, respectively, depending on Reynolds number. At the same Reynolds number, the thermal performance factors given by PDTs with $l/y$ = 0.5, 0.75 and 1.0 were higher than those given by ST, by around 17.5%, 15.9% and 14.5%, respectively, and higher than those given by DTs by about 2.8%, 1.5% and 0.2%, respectively. The PDTs with the smallest cutting pitch ratio ($l/y$ = 0.5) gave thermal performance factor higher than the ones with $l/y$ = 0.75 and 1.0 by around 1.3% and 2.6%, respectively. It should be mentioned that thermal performance factors associated with the use of all PDTs were above unity when Reynolds numbers were below 10,000. These results demonstrate the benefit of using PDTs with small cutting pitch ratios at low Reynolds numbers.

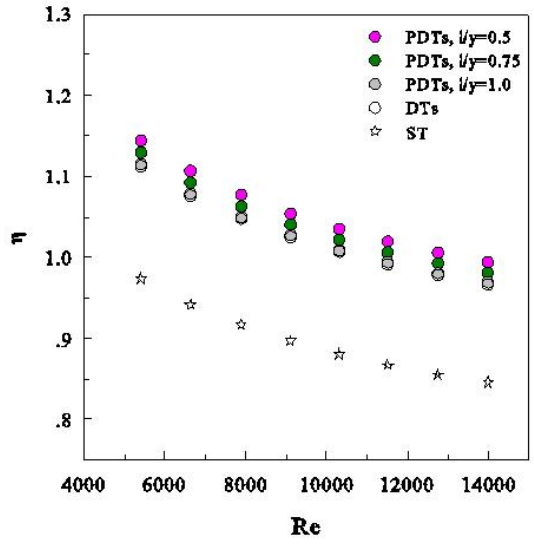


**Figure 9:** Thermal performance factor against Reynolds number for PDTs at various cutting pitchratios ($l/y$ = 0.5, 0.75 and 1.0).

## 5.5 Empirical correlation

One objective of the present work was to develop an empirical correlations for predicting Nusselt number, friction factor and thermal performance factor of tubes equipped with PDTs. These correlations were developed by log-linear regression analysis. The influential effects that were taken into account for the developing correlations included: (1) the thermal boundary condition; (2) the peripherally-cut dual twisted tapes (PDTs) geometry and (3) fluid property variation across the boundary layer. The correlations of Nusselt number and friction factor were developed for use under uniform wall heat flux boundary and isothermal conditions, respectively. Resultant correlations for predicting Nusselt number, friction factor and thermal performance factor are given below:

$$Nu = 0.351\, Re^{0.608} Pr^{0.4} \left(1 + \frac{1}{y}\right)^{-0.265} \tag{19}$$

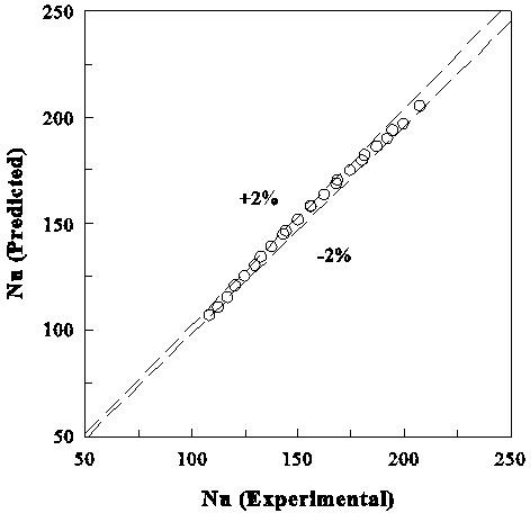


**Figure 10:** Comparison between predicted and experimental Nusselt numbers.

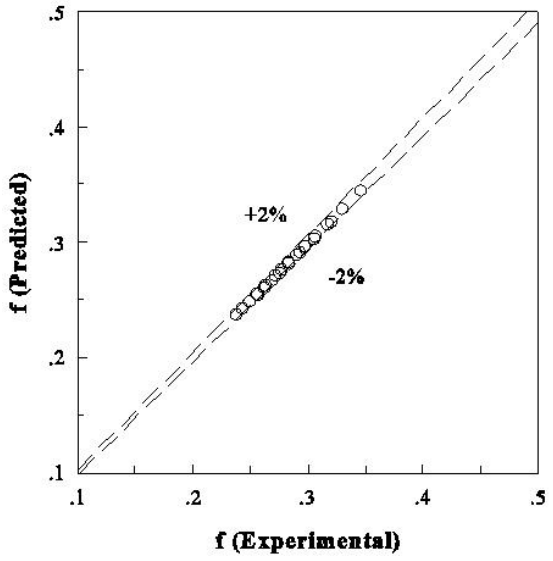


**Figure 11:** Comparison between predicted and experimental friction factors.

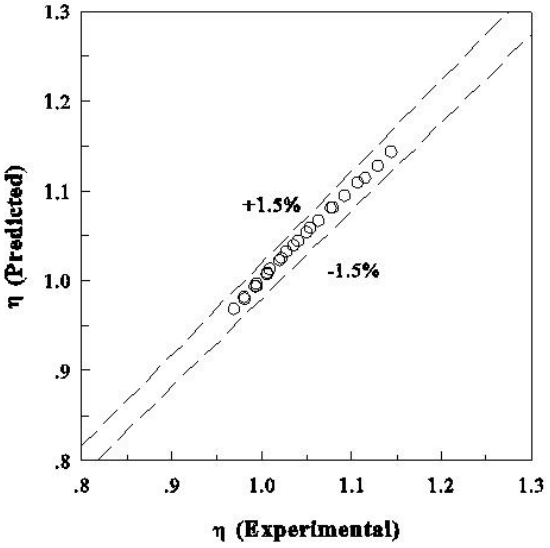


**Figure 12:** Comparison between predicted and experimental thermal performance factors.

$$f = 3.194\, Re^{0.234} \left(1 + \frac{1}{y}\right)^{0.168-0.529} \tag{20}$$

$$\eta = 4.23\, Re^{-0.148} \left(1 + \frac{1}{y}\right)^{-0.089} \tag{21}$$

The predicted Nusselt numbers, friction factors and thermal performance factors for turbulent flow obtained using Eq. 19 to 21 were compared with experimental values, as shown in Figures 10 to 12. Evidently, the predicted and experimental data were in good agreement, with deviations within ±2 for Nusselt number, ±2 for friction factor and ±1.5 for thermal performance factor.

# 6 Conclusions

The major findings of the present investigation can be summarized as follows:

1. Peripherally-cut dual twisted tapes (PDTs) performed better than the typical dual twisted tapes (DTs) and single twisted tape (ST) for heat transfer enhancement.
2. For the tested PDTs, the ones with smaller cutting pitch ratio ($l/y$) gave higher Nusselt numbers, friction factors and thermal performance factors.
3. The PDTs with $l/y = 0.5$, 0.75 and 1.0 offered, respectively, thermal performance factors between 0.99 and 1.14, 0.98 and 1.13, and 0.97 and 1.11,for Reynolds number ranging from 5400 to 14,000.
4. For the range considered, the thermal performance factor of 1.14 was achieved by using PDTs with the smallest cutting pitch ratio ($l/y = 0.5$) and the lowest Reynolds number of 5400. This demonstrates the benefit of using PDTs with small cutting pitch ratios at low Reynolds numbers.
5. In addition, empirical correlations of Nusselt number, friction factor and thermal performance factor were formulated from the experimental results of the tubes with PDTs.

**Acknowledgement:** This work was financially supported by the Energy Policy and Planning Office, Ministry of Energy, Thailand (EPPO).

# Nomenclature

| | |
|---|---|
| $A$ | heat transfer surface area, [$m^2$] |
| $C_p$ | specific heat of fluid, [J $kg^{-1}$ $K^{-1}$] |
| $D$ | inside diameter of the test tube, [m] |
| $f$ | friction factor, [-] |
| $h$ | heat transfer coefficient, [W $m^{-2}$ $K^{-1}$] |
| $I$ | current, [A] |
| $k$ | thermal conductivity of fluid, [W $m^{-1}$ $K^{-1}$] |
| $l$ | cutting pitch, [m] |
| $L$ | length of the test section, [m] |
| $M$ | mass flow rate, [kg $s^{-1}$] |

| | |
|---|---|
| $Nu$ | Nusselt number, [-] |
| $P$ | pressure of flow in stationary tube, [Pa] |
| $\Delta P$ | pressure drop, [Pa] |
| $Pr$ | Prandtl number, [-] |
| $Q$ | heat transfer rate, [W] |
| $Re$ | Reynolds number, [-] |
| $t$ | thickness of the test tube, [m] |
| $T$ | temperature, [K] |
| $\tilde{T}$ | mean temperature, [K] |
| $U$ | mean axial flow velocity, [m $s^{-1}$] |
| $V$ | voltage, [V] |
| $W$ | twisted tape width, [m] |
| $y$ | twisted tape pitch, [m] |
| $x$ | point or local, [-] |
| $X_i$ | $i^{th}$ variable, [-] |

Greek letters

| | |
|---|---|
| $\rho$ | fluid density, [kg $m^{-3}$] |
| $\delta$ | twisted tape thickness, [m] |
| $\mu$ | fluid dynamic viscosity, [kg $s^{-1}$ $m^{-1}$] |
| $\eta$ | thermal performance factor, [-] |
| $\delta R$ | uncertainty in the result, [-] |

Subscripts

| | |
|---|---|
| $b$ | bulk |
| $c$ | convection |
| $i$ | inlet |
| $o$ | outlet |
| $p$ | plain |
| $s$ | surface |
| $t$ | twisted tape |
| $w$ | water |

Abbreviations

| | |
|---|---|
| ST | typical single twisted tape |
| DTs | typical dual twisted tapes |
| PDTs | peripherally-cut dual twisted tapes |

# References


[1] Abdul Rasool A. A., Hamad F. A., Flow structure and cooling behavior of air impingement on a target plate, Central European J. Eng., 2013, 3, 400-409.

[2] Srinivasacharya D., Upendar M., Soret and dufour effects on MHD mixed convection heat and mass transfer in a micropolar fluid, Central European J. Eng., 2013, 3, 679-689.

[3] Hajmohammadi M. R., Eskandari H., Saffar-Avval M., Campo A., A new configuration of bend tubes for compound optimization of heat and fluid flow, Energy 2013, 62, 418-424.

[4] Hajmohammadi M. R., Nourazar S. S., Campo A., Poozesh S., Optimal discrete distribution of heat flux elements for in-tube laminar forced convection, International Journal of Heat and Fluid Flow, 2013, 40, 89-96.

[5] Hajmohammadi M. R., Poozesh S., Rahmani M., Campo A., Heat transfer improvement due to the imposition of non-uniform wall heating for in-tube laminar forced convection, Applied Thermal Engineering, 2013, 61, 268-277.

[6] Hajmohammadi M. R., Rahmani M., Campo A., JoneydiShariatzadeh O., Optimal design of unequal heat flux elements for optimized heat transfer inside a rectangular duct, Energy, 2014, 68, 609-616.

[7] Guo J., FanA., Zhang X., Liu W., A numerical study on heat transfer and friction factor characteristics of laminar flow in a circular tube fitted with center-cleared twisted tape, Int. J. Thermal Sciences, 2011, 50, 1263-1270.

[8] Bas H., Ozceyhan, Heat transfer enhancement in a tube with twisted tape inserts placed separately from the tube wall, Experimental Thermal and Fluid Science, 2012, 41, 51-58.

[9] Eiamsa-ard S., Somkleang P., Nuntadusit C., Thianpong C., Heat transfer enhancement in tube by inserting uniform/non-uniform twisted-tapes with alternate axes: Effect of rotated-axis length, Applied Thermal Engineering, 2013, 54, 289-309.

[10] Eiamsa-ard S., Thianpong C., Eiamsa-ard P., Turbulent heat transfer enhancement by counter/co-swirling flow in a tube fitted with twin twisted tapes, Experimental Thermal and Fluid Science, 2010, 34, 53-62.

[11] Eiamsa-ard S., Wongcharee K., Single-phase heat transfer of CuO/water nanofluids in micro-fin tube equipped with dual twisted-tapes, Inter. Comm. Heat and Mass Transfer, 2012, 39, 1453-1459.

[12] Hong Y., Deng X., Zhang L., 3D Numerical study on compound heat transfer enhancement of converging-diverging tubes equipped with twin twisted tapes, Chinese Journal of Chemical Engineering, 2012, 20, 589-601.

[13] Promvonge P., Pethkool S., Pimsarn M., Thianpong C., Heat transfer augmentation in a helical-ribbed tube with double twisted tape inserts, Inter. Comm. Heat and Mass Transfer, 2012, 39, 953-959.

[14] Eiamsa-ard S., Wongcharee K., Heat transfer characteristics in micro-fin tube equipped with double twisted tapes: Effect of twisted tape and micro-fin tube arrangements, J. Hydrodynamics, Ser. B, 2013, 25, 205-214.

[15] Bhuiya M. M. K., Sayem A. S. M., Islam M., Chowdhury M. S. U., Shahabuddin M., Performance assessment in a heat exchanger tube fitted with double counter twisted tape inserts, Inter. Comm. Heat and Mass Transfer, 2014, 50, 25-33.

[16] Moffat R. J., Describing the uncertainties in experimental results, Experimental Thermal Fluid Science, 1988, 1, 3-17.

[17] Gül H., Evin D., Heat transfer enhancement in circular tubes using helical swirl generator insert at the entrance, Int. J. Thermal Sciences, 2007, 46, 1297-1303.

[18] Petukhov B. S., Heat transfer and fraction in turbulent pipe flow with variable physical properties, in: Advances in Heat Transfer, 1970, 6, 504-564.

[19] Bilen K., Akyol U., Yapıcı S., Heat transfer and friction correlations and thermal performance analysis for a finned surface, Energy Conversion and Management, 2001, 42, 1071-1083.